Non-adiabatic interaction of ions with solar wind discontinuities

Alexander Vinogradov[1,2], Anton Artemyev[1,3], Ivan Vasko[1,4], Alexei Vasiliev[1] , and Anatoly Petrukovich[1]

[1]Space Research Institute RAS, Space Plasma, Moscow, Russia

[2]Higher School of Economics, Faculty of Physics, Moscow, Russia

[3]University of California in Los Angeles, Los Angeles, USA

[4]Space Sciences Laboratory, University of California, Berkeley, USA

Solar wind

The solar wind is the supersonic flow of magnetized plasma that can be fast (V ~ 500 - 800 km/s) or slow (V ~ 300 - 500 km/s).

- The problem of solar wind heating
- Current sheets contributes significantly to the spectrum of magnetic turbulence, and thus can be important for solar wind heating

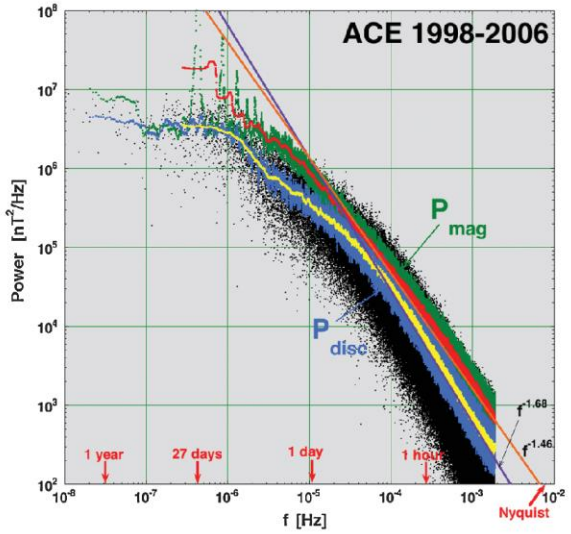

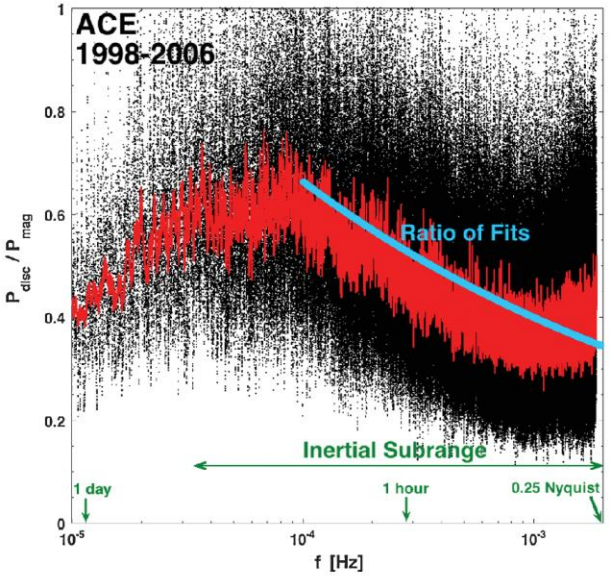

Joseph E. Borovsky Phys. Rev. Lett. 2010

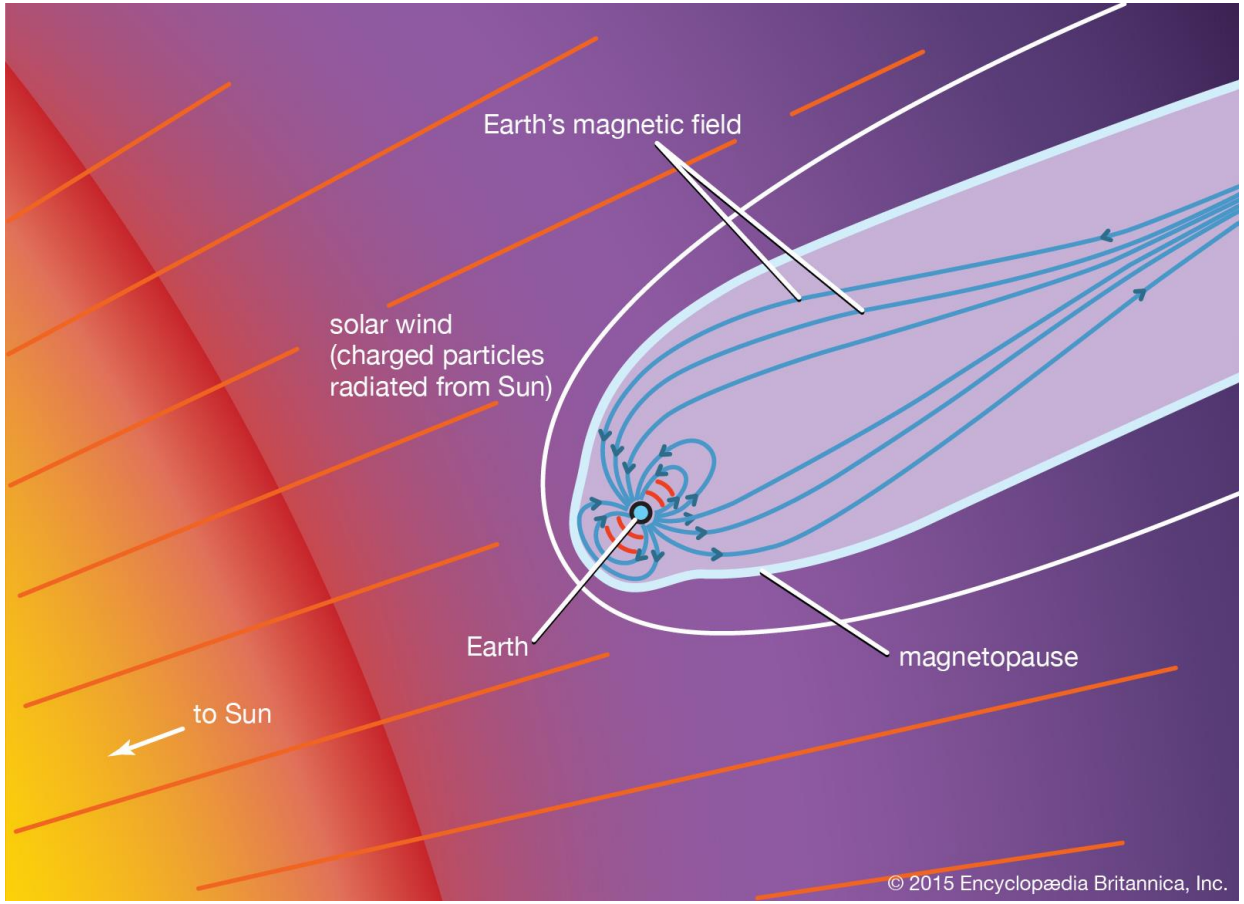

Symbol	Solar wind	(Upper) Corona	Definition
n_p, n_e	$3\,\mathrm{cm}^{-3}$	$10^6\,\mathrm{cm}^{-3}$	Proton and electron number density
T_p, T_e	10^5 K	10^6 K	Proton and electron temperature
B	3×10^{-5} G	1 G	Magnetic field strength

Solar wind parameters
Verscharen, D., Klein, K.G. & Maruca, B.A. The multi-scale nature of the solar wind. *Living Rev Sol Phys* **16,** 5 (2019)

MHD classification of discontinuities

Previous works have seen 100-200 discontinuities per day.

MHD classification:

Rotational discontinuities:

formed by the Alfven waves in heterogeneous plasma

Tangential discontinuities:

formed at the borders of solar wind flows at different speeds

Consider ion dynamics in rotational solar wind discontinuities.

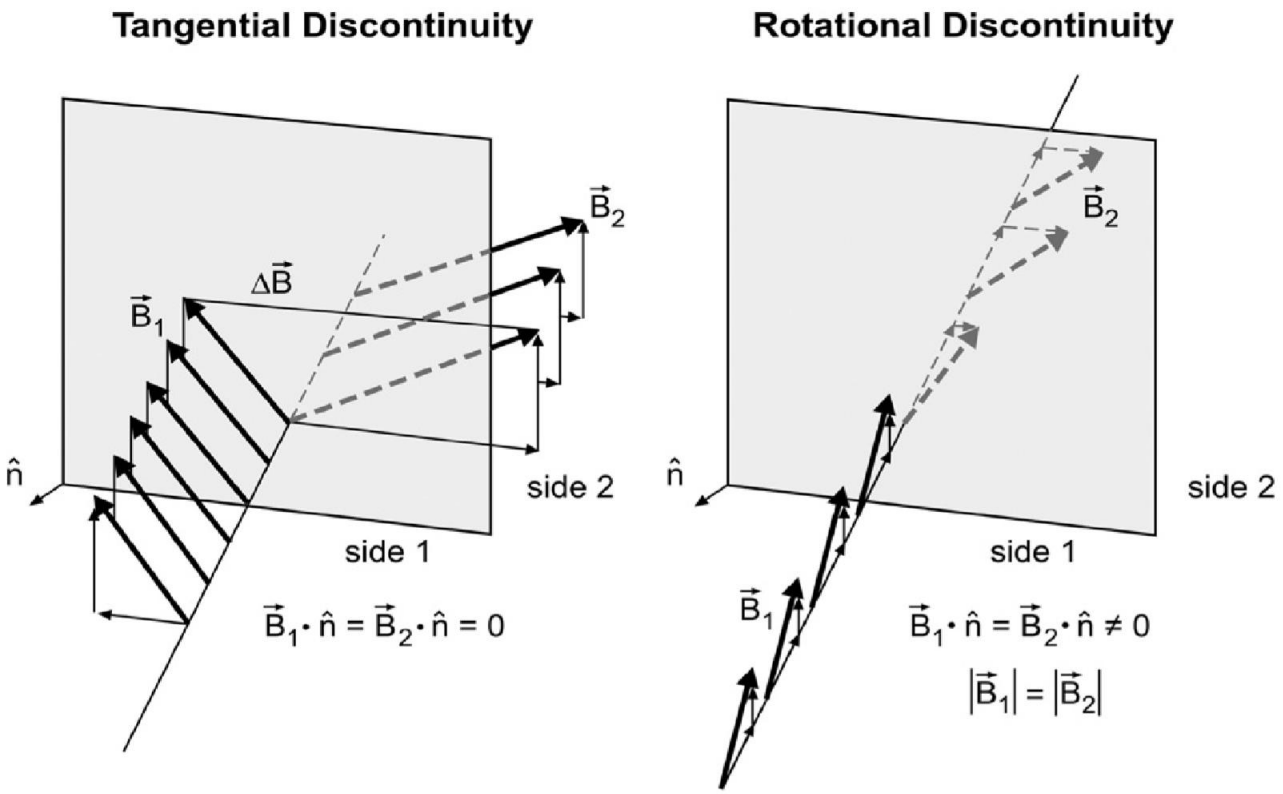

Tsurutani B.T. et al. A review of interplanetary discontinuities and their geomagnetic effects (2011)
Hudson P.D. Discontinuities in an anisotropic plasma and their identification in the solar wind (1970)

MMS observations of the solar wind current sheets

- Occurrence rate ~140 current sheets per day

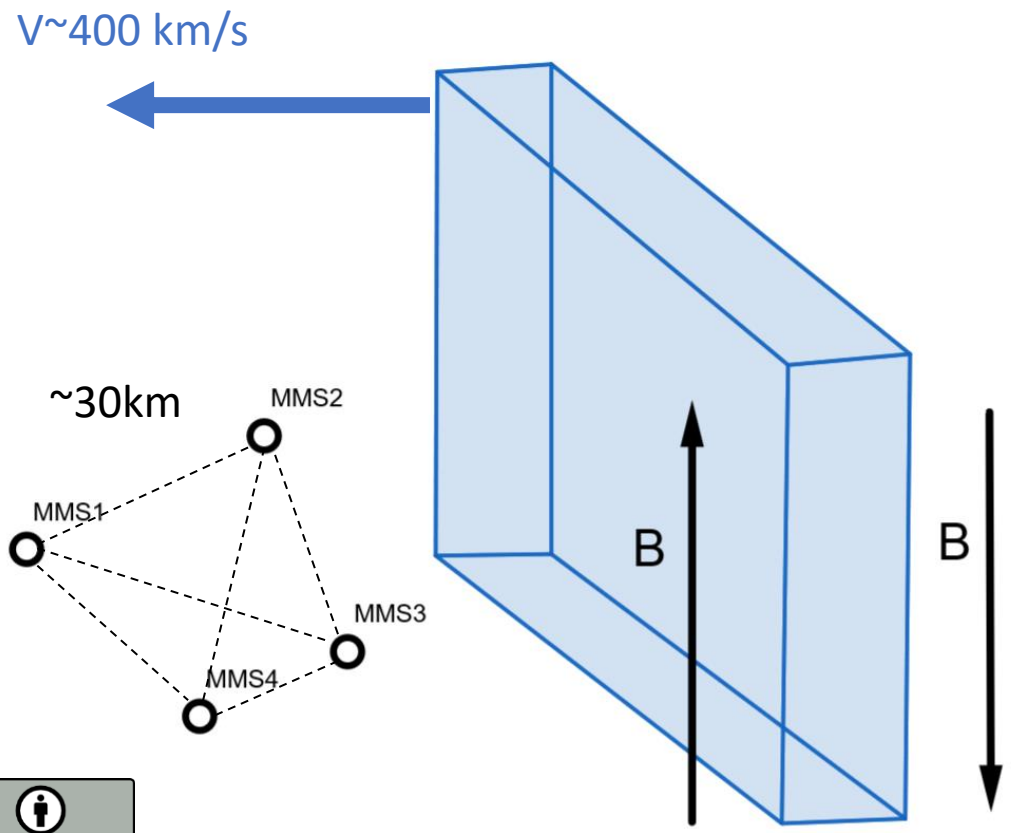

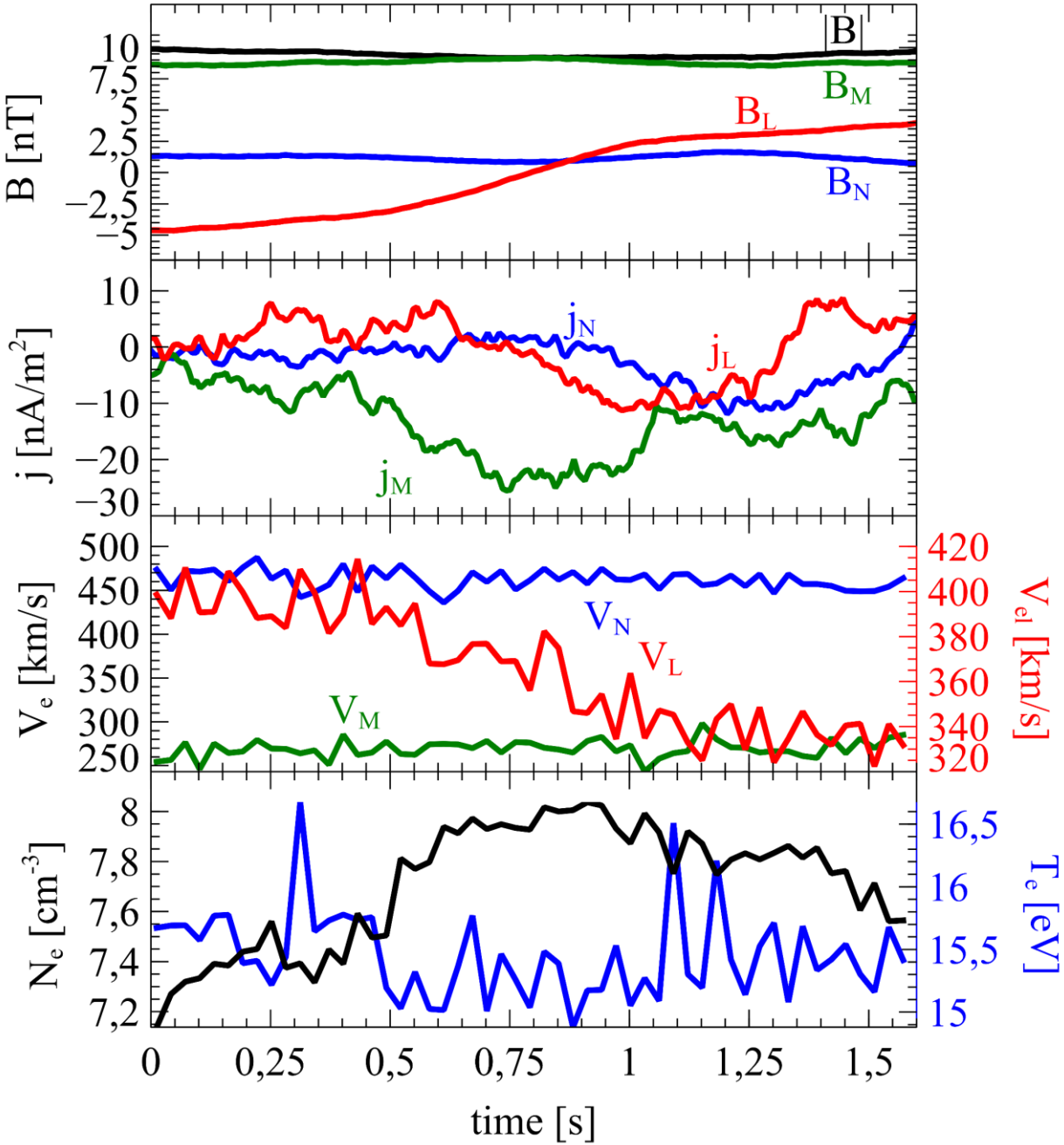

CS thickness and current density distributions according to MMS observation statistics

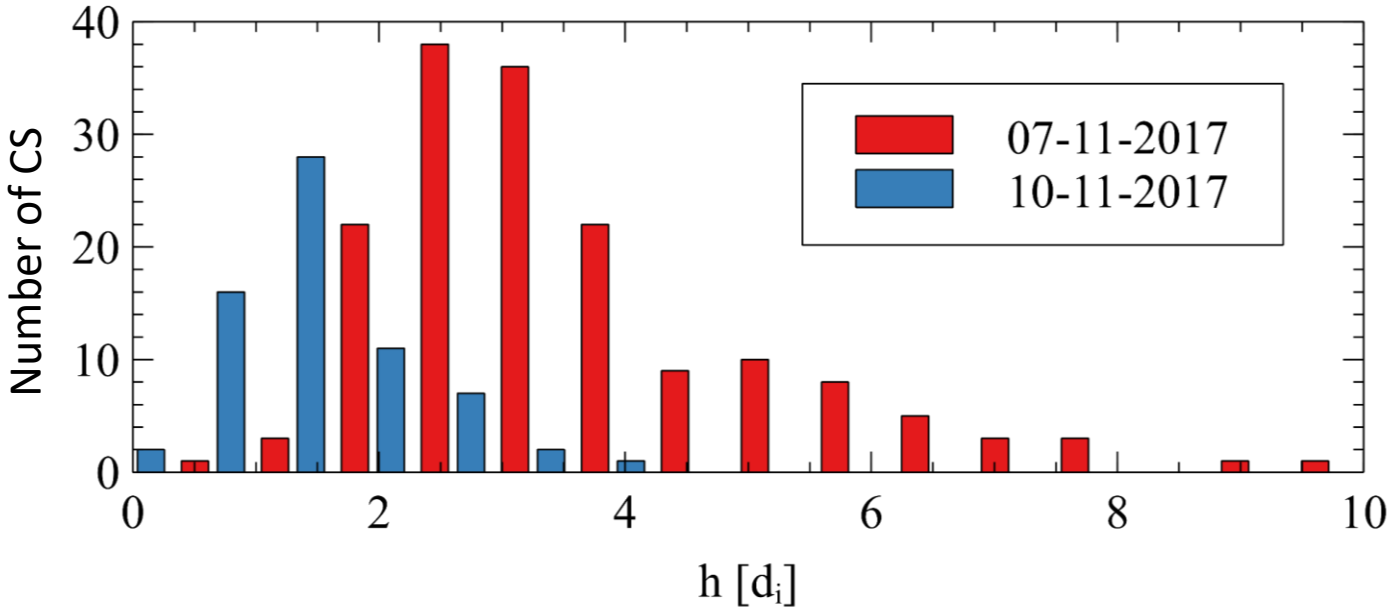

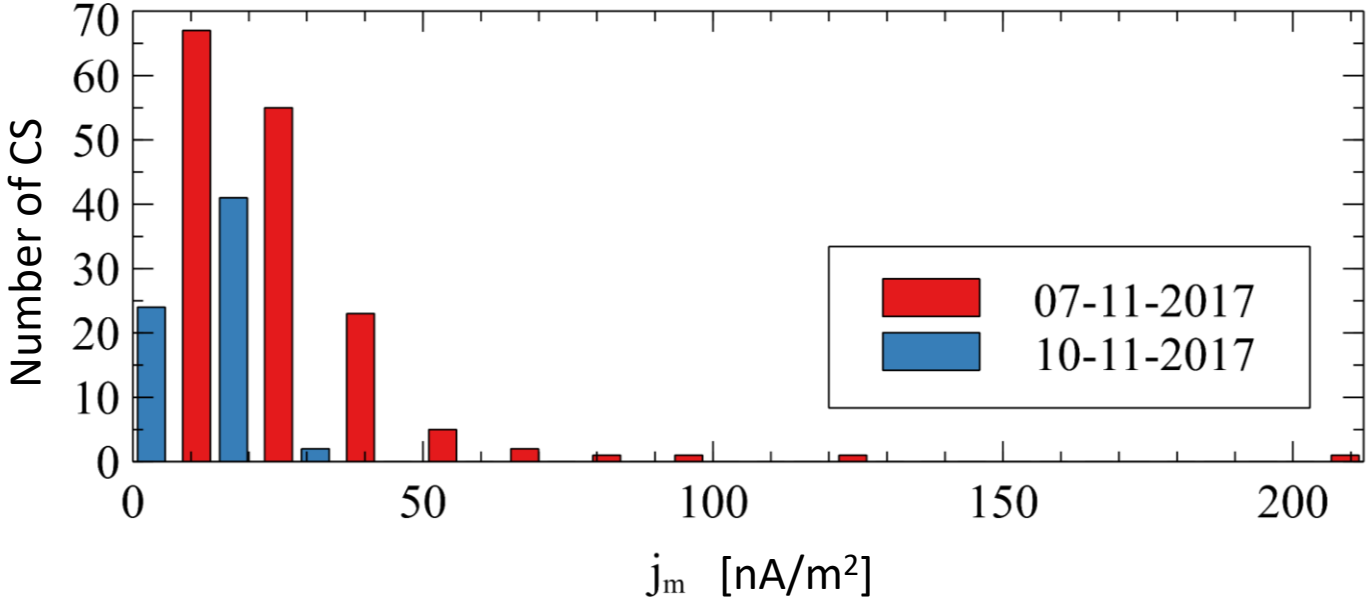

Current sheet thickness shows that these are kinetic-scale structures. Such structures should effectively scatter ions!

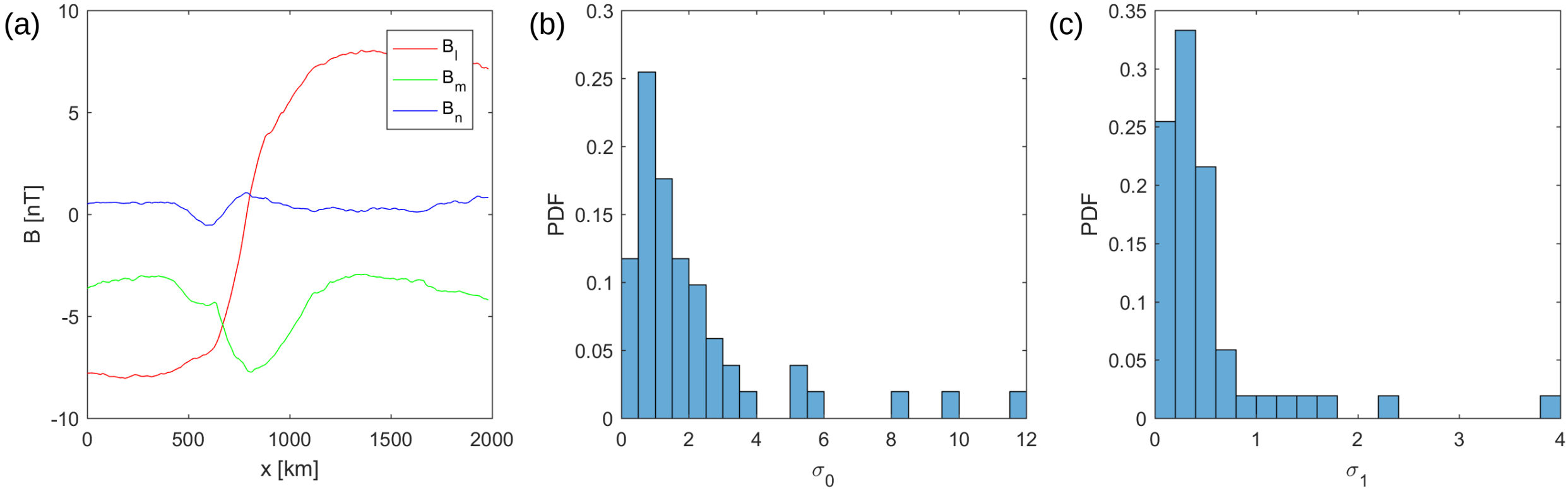

(a) Typical example of solar wind current sheet (discontinuity). Three magnetic field components are shown in the local coordinate system: B_l is the reversing magnetic field component, B_n is the component normal to the discontinuity surface, B_m is the component peaking at the discontinuity center. Coordinate n along the normal to the discontinuity surface is reconstructed using the timing technique.

We introduce a simple magnetic field model approximating the main discontinuity characteristics: B_l reversal, B_m peak and constant values at the discontinuity boundary, constant B_n:

$$B_x = B_0 tan\,h\left(\frac{z}{L}\right), B_y = \frac{\sigma_1 B_0}{cosh\left(\frac{z}{L}\right)} + \sigma_0 B_0, B_z = const$$

Figures (b) and (c) show the distribution of σ_0 and σ_1 parameters for the statistics of observed discontinuities.

Ion interaction with the current sheet

In the reference frame $p_y = 0$ Hamiltonian has the following form:

$$H = \frac{1}{2}\left[p_x + \frac{2\sigma_1}{\eta^2}\left(arctan(exp(-\eta z)) - \frac{\pi}{4}\right) - \sigma_0 \eta z\right]^2 + \frac{1}{2}\left[\kappa x - \frac{1}{\eta^2} log(cosh(\eta z))\right]^2 + \frac{1}{2}p_z^2$$

Parameters: $\kappa = \frac{B_z}{B_0}\sqrt{\frac{L}{\rho_0}} = \sqrt{\frac{R_c}{\rho_0}} < 1$ - crucial parameter controlling the efficiency of such scattering, the ratio of magnetic field line curvature radius and ion Larmor radius

$\eta = \sqrt{\frac{\rho_0}{L}}$ $\rho_0 = \frac{\sqrt{2Hm}c}{eB_0}$ - Larmor radius, L – CS scale

For small κ, the Hamiltonian equations of motion consist of two pairs of equations for slow ($\kappa x, p_x$) and fast (z, p_z) variables:

Slow variables: ($\kappa x, p_x$)

$$\begin{cases} \frac{dp_x}{dt} = -\kappa \frac{\partial H}{\partial \kappa x} \\ \frac{d\kappa x}{dt} = \kappa \frac{\partial H}{\partial p_x} \end{cases}$$

Fast variables: (z, p_z)

$$\begin{cases} \frac{dp_z}{dt} = -\frac{\partial H}{\partial z} \\ \frac{dz}{dt} = \frac{\partial H}{\partial p_z} \end{cases}$$

Jump of I_z

Ion dynamics on the plane of fast variables is the oscillation in a potential well.

$$I_z = \sqrt{2}\oint \sqrt{H - U(z, \kappa x, p_x)}dz$$

I_z is conserved with exponential accuracy $\sim \exp(-1/\kappa^2)$, and thus $I_z(\kappa x, p_x)$=const determines a particle trajectory in the $(\kappa x, p_x)$ plane. However, z-oscillations in U potential can be significantly changed due to the evolution of U shape, and such changes result in dynamical $\sim$ O(κ) and geometrical $\sim$ O(1) jumps of I_z

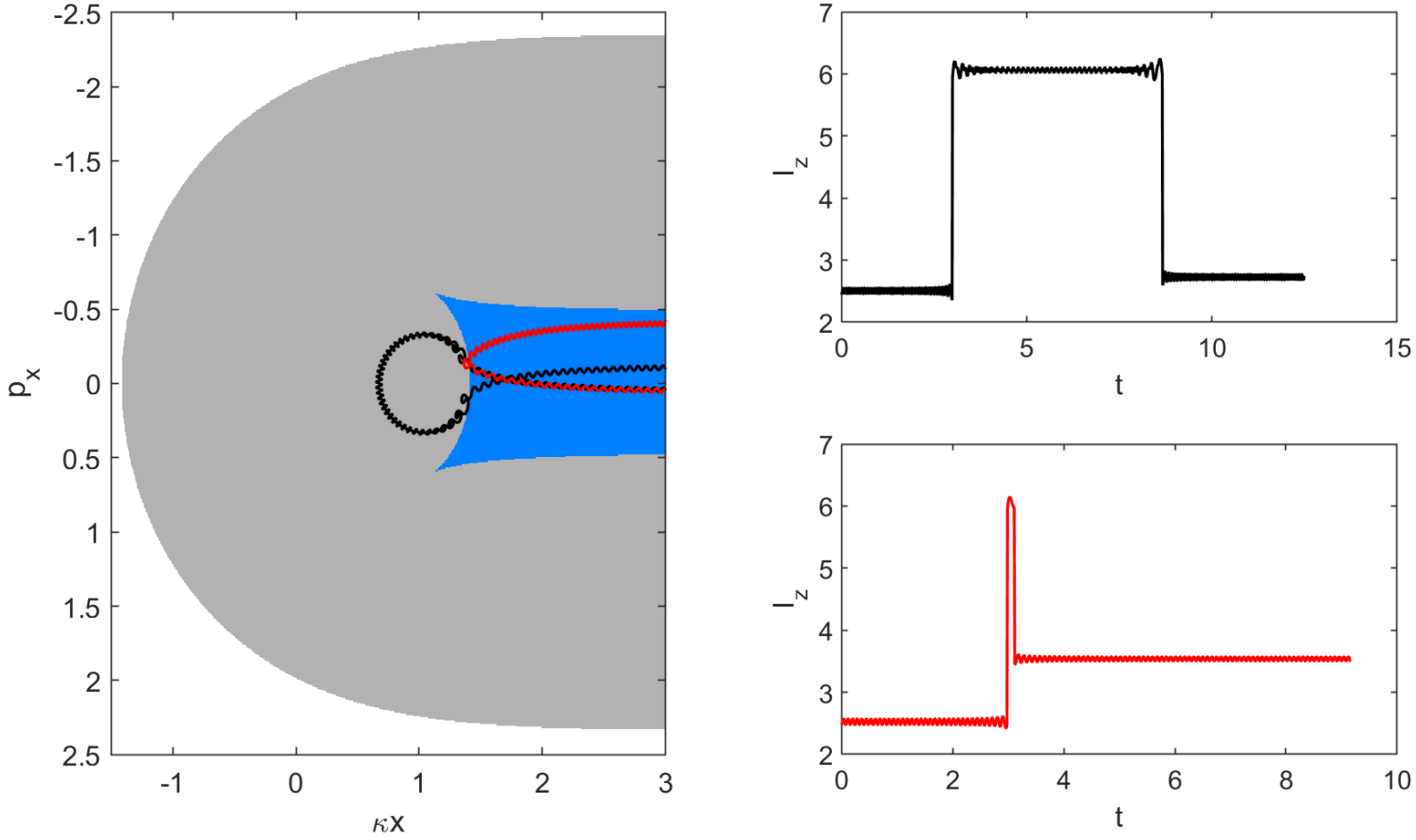

Figure shows two trajectories calculated at small $\kappa = 10^{-2}$, so dynamical I_z jumps for these trajectories are negligible. The red trajectory approaches the boundary between the blue and grey areas and reflects from this boundary (reflects from the current sheet), whereas the black trajectory crosses this boundary twice (makes a rotation within the current sheet). Both reflections and crossings imply change of U shape and should correspond to I_z jumps. Indeed, right panels shows I_z jumps for these two trajectories: there is a significant I_z change between the initial and final states, and these changes are much larger than expected dynamical jumps ~O(κ). Therefore, there are geometrical jumps in the system described with Hamiltonian.

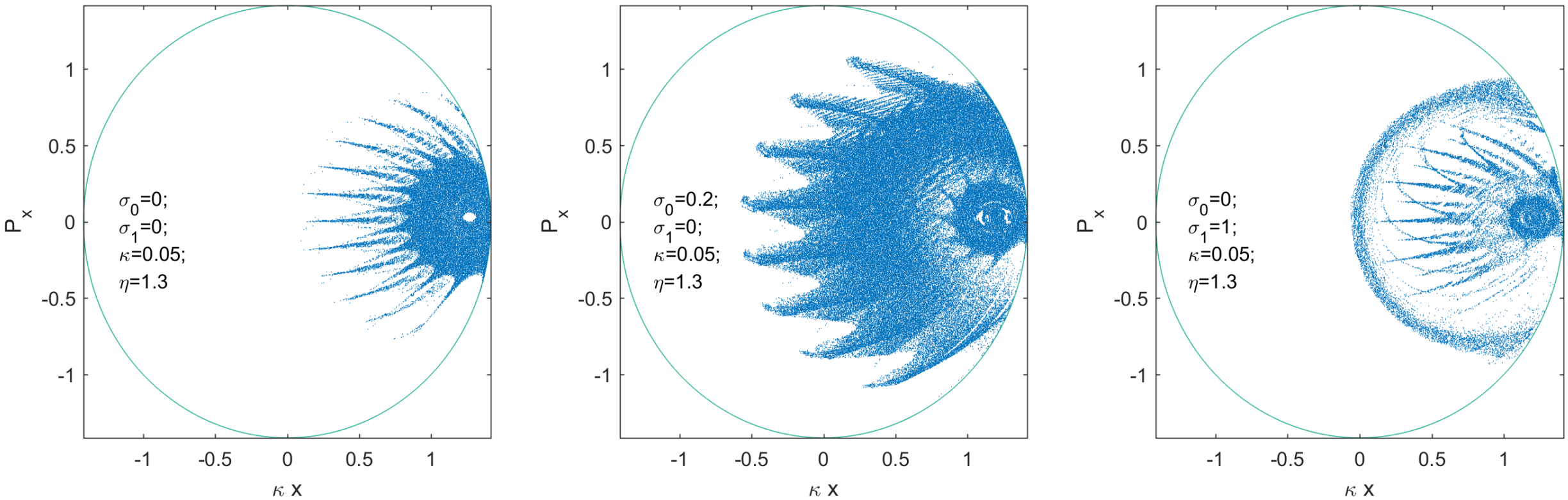

- Figure shows three Poincaré maps for Hamiltonian: without B_m field ($\sigma_{0,1}$= 0), with constant B_m (σ_1= 0), and with B_m peak (σ_0= 0).
- For B_m = 0 system we obtain large population of initially transient trajectories (empty space in the (κx,px) plane) and large region of initial B_m corresponding to quasi-trapped trajectories (random dots in the (κx,px) plane).
- The quasi-trapped trajectory region significantly larger in the system with constant B_m (i.e., with σ_0= 0). This is an effect of particle trajectory splitting in such system: due to geometrical jumps I_z value of each particle regularly changes, but for each trajectory the set of these changes is finite and the changes are not random, i.e. there are several I_z values for each trajectory, but such Iz jumps do not result in the particle escape from the system.
- The most interesting Poincaré map can be seen for the system with B_m peak (σ_1= 0): area of quasi-trapped trajectory region significantly shrinks and there are a lot of particles escaping from the system due to I_z geometrical jumps (empty area between the two regions filled with random dots). This is the new effect of particle scattering away from the system by rapid I_z destruction.

I_z scattering matrix B_y

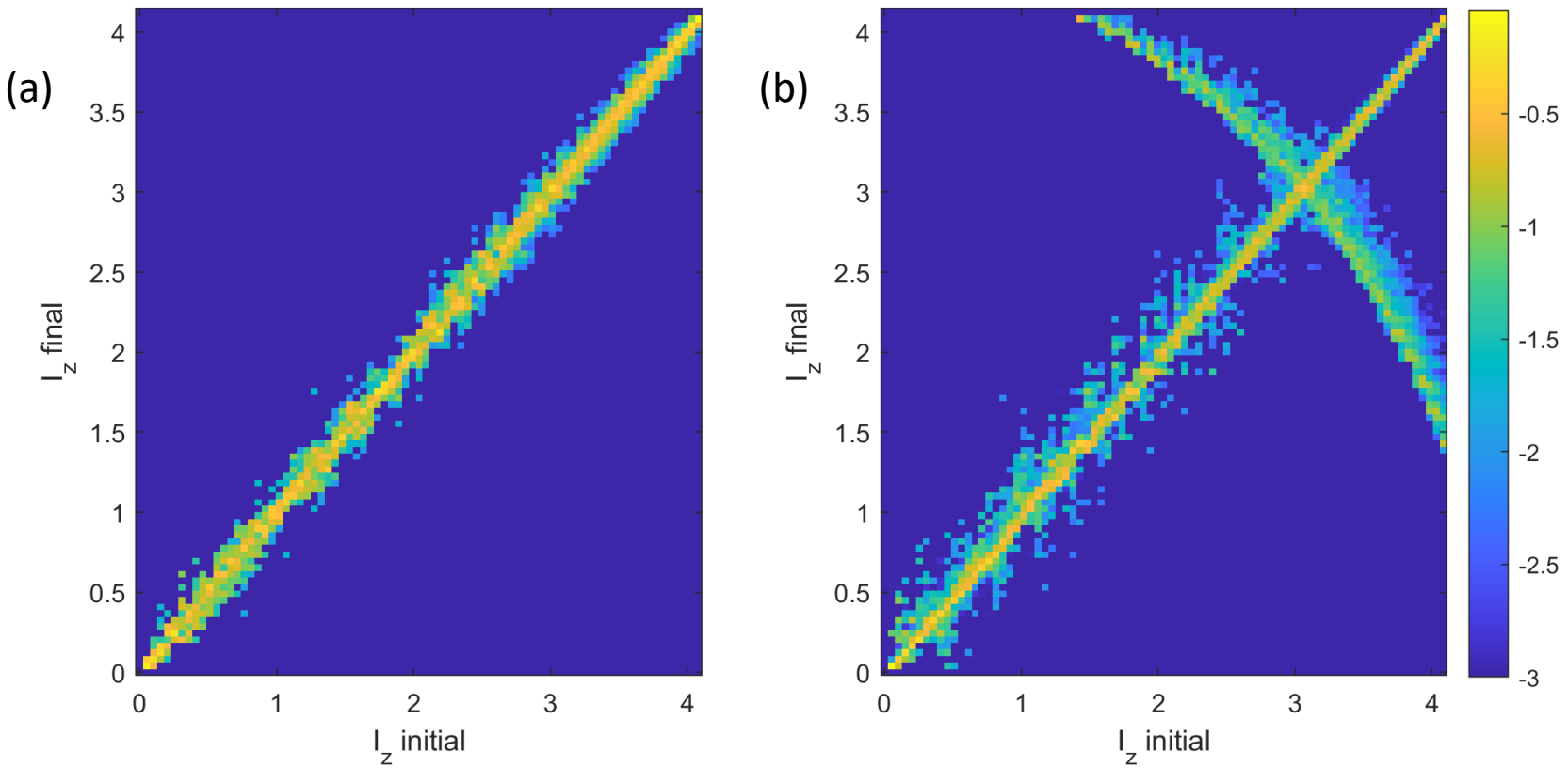

We run $\sim 10^3$ trajectories from the system boundary κx=4 for each initial I_z and then, when particles come back to this boundary, we calculate B_m final. Therefore, for each initial I_z we have a distribution of final I_z and such distributions form the transformation matrix in (I_z initial, I_z final) space. Figure compares these matrices for Hamiltonian with B_m = 0 (left panel) and with B_m peak (right panel). In absence of B_m the matrix is almost diagonal with small spread around $I_{z,initial}$ = $I_{z,final}$ (this spread is due to small dynamical jumps). For the system with B_m peak the matrix demonstrates significant probability for large change in I_z additional to the diagonal, there is a cross-diagonal structure in the matrix.

Conclusion

- The interaction of ions with kinetic scale current sheets corresponding to MMS observations in the solar wind has been studied
- In this study we show how the B_y peak affects ion scattering on discontinuities. The numerical study of trajectories showed that sharp jumps of quasi-adiabatic invariant occur when the ions are scattered on a layer with a bell-shaped field B_y
- The quasi-adiabatic invariant destruction should result in rapid ion scattering (and heating in case of electric field presence in the current sheet reference frame)